Nonlinear spin-charge dynamics in a driven double quantum dot

D. V. Khomitsky[1] and E. Ya. Sherman[2]
[1]*Department of Physics, University of Nizhny Novgorod, 23 Gagarin Avenue, 603950 Nizhny Novgorod, Russian Federation*
[2]*Departamento de Química Física, Universidad del País Vasco–Euskal Herriko Unibertsitatea, 48080 Bilbao, Spain*
(Received 3 April 2009; revised manuscript received 22 May 2009; published 22 June 2009)

The coupled nonlinear coordinate and spin dynamics of an electron in a double quantum dot with spin-orbit interaction is studied semiclassically. The system is driven by an electric field with the frequency matching the orbital or the Zeeman resonance in magnetic field. Calculated evolution of the spin state is crucially sensitive to the irregularities in the spatial motion and the geometry of the host nanostructure. The resulting spin-flip Rabi frequency has an unusual dependence on the field amplitude, demonstrating an approach to the chaotic spin motion. In turn, the orbital dynamics depends strongly on the spin evolution due to the spin-dependent term in the electron velocity.

DOI: 10.1103/PhysRevB.79.245321 PACS number(s): 73.63.Kv, 72.25.Dc, 72.25.Pn

I. INTRODUCTION

Spins of electrons confined in nanostructures show a rich coherent and dissipative dynamics (for example, Refs. 1–3) which should be taken into account for the fundamental understanding of their properties and possible application in quantum information[4] and spin-dependent charge transport. The spin-orbit (SO) coupling, which usually manifests itself in low-dimensional systems as the linear in the electron momentum effective field acting on electron spin, is one of the main causes of this richness. This momentum-dependent coupling offers a new way of manipulating the electron spin by influencing the electron momentum, that is, by an external periodic electric field. This effect, the electric-dipole spin resonance,[5] is in the basis of the very promising proposal of Rashba and Efros[6] for spin manipulation of electrons confined by and external potential in lateral quantum dots (QDs) on the spatial scale of the order between 10 and 100 nm. The weak coupling of the electric field to the spin is sufficient to manipulate spins of confined in QDs electrons and holes[7] and produce inhomogeneous spin patterns in lateral semiconductor structures.[8] The efficiency of this technique was demonstrated experimentally with the single-electron QDs.[9,10] Another side of this coupling is the influence of the spin state and dynamics on the charge motion. This effect studied experimentally and theoretically (see, for example, Refs. 11–13) is important, especially when it is accumulated at long times leading to qualitatively new transport phenomena or transitions of the system to well-separated final states. The feedback SO coupling effect in the electron-weak localization was considered in Refs. 14 and 15. Relaxation of spin states due to the coupling to the environment[16,17] strongly limits the abilities to initialize, keep, and manipulate the desired spin states.

A fast spin manipulation often on the time scales strongly limited by the spin-relaxation times requires a relatively large electric field amplitude. This electric field, in turn, can strongly influence the orbital dynamics and drive the system far beyond the linear motion in the confining potential.

A single QD can be well described by a two-dimensional parabolic or elliptic potential; however, considerably more complex systems are required for applications, such as—at least—double quantum dots with a double minimum potentials. Taking into account the interest in spin systems in electric field, the full coupled dynamics of the spin and coordinate degrees of freedom in a driven QD deserves analysis and understanding of the operation regimes. One of the central questions arising in such a dynamical problem for multiminima potentials is the irregularity and possible transition to the classical and quantum chaos not only for the coordinate[18–20] but also for spin. The problems which has to be addressed are how possible irregularities and chaos in the orbital motion influence the spin dynamics and what effects in the charge dynamics can be caused by the corresponding irregular spin motion? The analysis of these effects aims on understanding the limits of the spin manipulation in nanostructures and set a link between spintronics and the nonlinear dynamics and chaos theories.

Most of the studies of spin dynamics in systems not driven by external field have been performed so far for the two-dimensional lateral QDs. However, one-dimensional (1D) systems, including quantum wires and wire-based QDs are of interest,[21–23] promising for the applications and can be treated by a thorough analysis of various double-QD problems.[23] In this paper, we concentrate on these systems, which demonstrate all important for the understanding features of the coupled spin-charge dynamics in driven systems.

II. SEMICLASSICAL MODEL FOR COUPLED DYNAMICS

As a model we consider a particle with mass m in a quartic potential

$$U(x) = U_0\left[-2\left(\frac{x}{d}\right)^2 + \left(\frac{x}{d}\right)^4\right], \tag{1}$$

describing a double-minimum system where the minima are separated by $2d$ in space with the barrier of U_0 in energy. Below we refer to this system as to the double-QD (DQD) system with each region $U(x)<0$ considered as a one-dimensional QD. For this potential, the classical[19] and quantum-tunneling-determined[20] dynamics driven by electric field have been studied. Here we concentrate on the classical

dynamics by considering mainly a wide structure with $d=100\sqrt{2}$ nm and $U_0=25$ meV. This high energy scale is on the order of 300 K, and, therefore, at temperatures below 100 K the orbital dynamics is only weakly sensitive to the temperature. For this reason, the thermal effects on the electron momentum and kinetic energy, including the spread and the activated over-the-barrier motion, will be neglected. The frequency of the single QD small-amplitude oscillations $\omega_0=2\sqrt{2}\sqrt{U_0/m}/d$ is 4.96×10^{12} s^{-1} at GaAs electron effective mass $m=0.067m_0$ (m_0 is the free-electron mass), the semiclassically calculated number of energy levels in a single QD $N_{E<0}=4\sqrt{2}d\sqrt{mU_0}/3\pi$ is close to eight, and the interdot semiclassical tunneling probability $\exp(-8\sqrt{2}\sqrt{mU_0}d/3)$ is vanishingly small, which allows to treat the dynamics semiclassically (we put $\hbar\equiv1$).

To characterize the SO interaction, we use the Dresselhaus type of coupling present in all the zincblend structures in the form

$$H_{\rm so}=\alpha_D(\boldsymbol{\kappa}\boldsymbol{\sigma}), \tag{2}$$

where α_D is the bulk Dresselhaus constant, $\boldsymbol{\sigma}$ are the Pauli matrices, $\kappa_x=\hat{p}_x(\hat{p}_y^2-\hat{p}_z^2)$ with other components obtained by the cyclic permutation, and p_i are the corresponding momentum components: $\hat{p}_x=-i\partial/\partial x$, etc. In a one-dimensional structure extended along the x axis, where the transverse motion is quantized, the Dresselhaus term is reduced to the linear in momentum term $\beta\sigma^x\hat{p}_x$, where $\beta=\alpha_D\langle\hat{p}_y^2-\hat{p}_z^2\rangle$ with the quantum-mechanical expectation value $\langle\hat{p}_y^2-\hat{p}_z^2\rangle$ for the ground state of the quantized transverse motion.[24] The value of β depends on the asymmetry of the system cross section and vanishes if it has a perfect square or circle shape. In the GaAs-based structures with the transverse dimensions of few nanometers, β is on the order of $0.1-0.5\times10^{-9}$ eV cm.

In the presence of the z-axis-oriented magnetic field B_z, the 1D Hamiltonian acquires the Zeeman term only and with the electric field $E(t)$ applied along the x axis it has the form

$$H=\frac{\hat{p}_x^2}{2m}+U(x)-eE(t)x+\beta\sigma^x\hat{p}_x+\frac{g}{2}\mu_B\sigma^zB_z. \tag{3}$$

Following the approach of Ref. 6, the direct Zeeman coupling of the magnetic field of the electromagnetic wave to the electron spin was neglected in Eq. (3). The evolution of mean values for variable X is governed by the equation of motion $\dot{X}=i[H,X]$ where [,] stands for the commutator. By applying the commutation rules for x, $\hat{p}_x$, and Pauli matrices, one obtains the following coupled equations for the coordinate and spin dynamics:

$$\dot{x}=p_x/m+\beta\sigma^x,$$

$$\dot{p}_x=-\partial U/\partial x+eE(t)-p_x/\tau_p,$$

$$\dot{\boldsymbol{\sigma}}=\{[\omega_{\rm so}\mathbf{x}+\mathrm{sgn}(g)\omega_L\mathbf{z}]\times\boldsymbol{\sigma}\}, \tag{4}$$

where $\omega_{\rm so}=2\beta p_x$, $\omega_L=|g|\mu_BB_z$ is the Larmor frequency, and $\mathbf{x}$, $\mathbf{z}$ are the unit vectors and upper dot stands for the time derivative. Since in the chosen range of parameters, the orbital (x,p_x) dynamic can be treated classically, here the momentum and coordinate are considered as the quantities governed by the classical equations of motion. We include here the momentum relaxation with $\tau_p=5$ ps being a typical relaxation time for the conduction electron. Since $\omega_0\tau_p\gg1$, this relaxation influences the dynamics weakly. Also, we neglect the spin relaxation which occurs on the time scales[25] much longer than the maximum times considered in this paper. Hence, the spin states studied here can be considered as long-standing spin states which properties are of particular importance for spintronics. The system (4) should be accompanied by the initial conditions for the position $x(0)$, momentum $p_x(0)$, and spin components $\sigma^i(0)$ which values are determined in real structures by the method of the spin-state preparation before the driving field is applied. The typical set of the initial parameters which we consider in the paper describes the spin-up electron located at the bottom of a particular quantum well.

III. DYNAMICS IN ELECTRIC FIELD

A. Zeeman resonance: $\omega=\omega_L$

To begin with, we consider analytically the resonance with $E(t)=-E_0\sin(\omega_Lt)$ at small E_0. For the moment, we suppose that $|e|E_0\ll U_0/d$, such that all nonlinear terms in the force acting on the electron are small compared to the linear ones and the orbital oscillations $x(t)$ are very close to the harmonic. Near the spin-flip resonance, we can consider the spin dynamics with the explicitly spin-dependent part of the Hamiltonian

$$H_s=\beta\sigma^x\hat{p}_x+\frac{g}{2}\mu_B\sigma^zB_z \tag{5}$$

in the two-level model, taking only the resonant contribution $\exp(-i\omega_Lt)$ in $\sin(\omega_Lt)=[\exp(i\omega_Lt)-\exp(-i\omega_Lt)]/2i$. In this rotating wave approximation, neglecting contributions of the off-resonance terms, Hamiltonian (5) can be written as

$$H_s=-\frac{1}{2}\begin{pmatrix}\omega_L & \Omega e^{i\omega_Lt}\\ \Omega e^{-i\omega_Lt} & -\omega_L\end{pmatrix} \tag{6}$$

with the Rabi frequency $\Omega=\beta p_R$, where $p_R=|eE_0|\omega_L/\omega_0^2$ is the amplitude of the driven momentum. The solution to the Schröedinger equation with Hamiltonian (6) yields

$$\langle\sigma^x\rangle=-\sin(\Omega t)\sin\omega_Lt,\quad \langle\sigma^y\rangle=-\sin(\Omega t)\cos\omega_Lt,$$

$$\langle\sigma^z\rangle=\cos(\Omega t). \tag{7}$$

The spin expectation values (7) show the Rabi oscillations in σ^z, while the amplitude of the σ^x and σ^y Larmor precession at ω_L is modulated with the Rabi frequency.

This analytical result can be compared to the numerical solution of system (4) with initial conditions corresponding to the spin-up electron in the left QD. Examples of σ^z dynamics and Fourier power spectra are shown in Fig. 1 for $g=-0.45$ (we assume the bulk GaAs value here), $\beta=0.2\times10^{-9}$ eV cm, and $B_z=4$ T corresponding to $\omega_L=1.6\times10^{11}$ s^{-1}. The power spectra v_{ω_m} were obtained as the Fourier transform of the numerical solution for the dynamical variables[26] $v(t=t_n)$ abd $n=1,\ldots,N$ of Eq. (4) at the frequen-

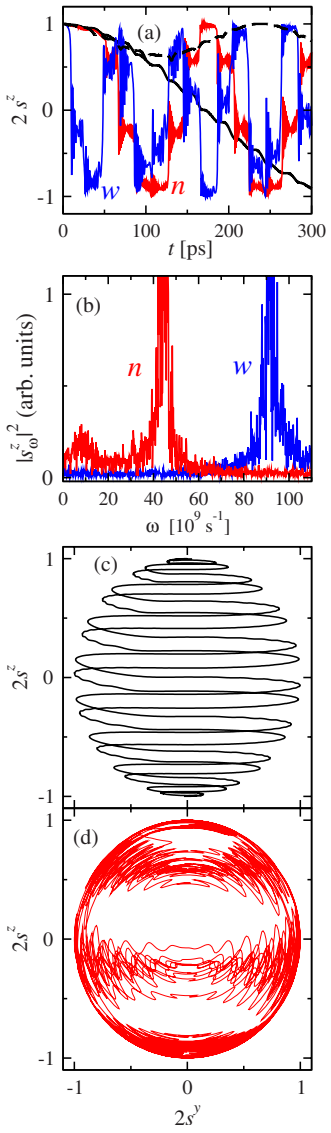

FIG. 1. (Color online) (a) Evolution of $\sigma^z(t)$ at $\omega=\omega_L$ for the confined motion in the left QD at $E_0=2.55$ kV/cm (solid black line) and $E_0=2.6$ kV/cm when the transfer is induced (line marked n, red) for the $d=100\sqrt{2}$ nm structure and for a structure with $d=200\sqrt{2}$ nm with the transfer at smaller $E_0=1.5$ kV/cm (line marked w, blue). Dashed black line shows $\sigma^z(t)$ at $E_0=2.55$ kV/cm, $d=100\sqrt{2}$ nm, and $\omega=1.1\omega_L$. The full spin flip is achieved only at the exact resonance. (b) Fourier transform spectra for $E_0=2.6$ kV/cm, $d=100\sqrt{2}$ nm (line marked n, red), $E_0=1.5$ kV/cm, and $d=200\sqrt{2}$ nm (line marked w, blue) showing the approach to the irregular spin dynamics. (c) Phase portrait for $\omega=\omega_L$, $d=100\sqrt{2}$ nm, $E_0=2.55$ kV/cm, and time $t<700$ ps. (d) Same for $E_0=2.6$ kV/cm.

cies $\omega_m=2\pi m/t_N$ defined by the overall time t_N of the observation

$$v_{\omega_m}=\sum_{n=1}^{N} v(t_n)e^{-2\pi i(n-1)(m-1)/N}. \tag{8}$$

The time dependence $\sigma^z(t)$ is shown in Fig. 1(a) for the exact Zeeman resonance $\omega=\omega_L$ for three cases illustrating different

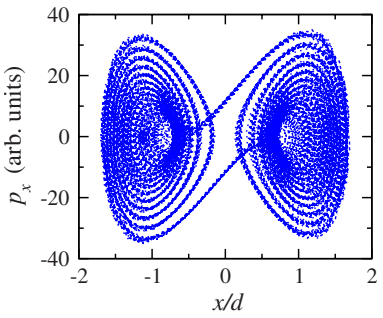

FIG. 2. (Color online) Phase portrait (x,p_x) of the system at $\omega=\omega_L$ and $E_0=2.6$ kV/cm when the transfer is possible at time $t<700$ ps. The pattern is dominated by the motion in a single (left or right) QD at the frequencies on the order of ω_0. The interdot transfer is a relatively rare event at the frequency ω_L.

regimes of the dynamics, the role of the structure geometry, and the effect of the interdot transfer for the spin dynamics and the Rabi frequency.

When the electron is still confined to one dot, the spin motion is regular and the Rabi frequency is approximately linear in the external field amplitude. When the amplitude is slightly increased from 2.55 to 2.6 kV/cm, the particle can travel through both QDs causing a strong change in the Rabi frequency and the entire spin dynamics. The Rabi frequency in this case is not related directly to ω_0 or the geometrically defined SO frequency $\omega_g=\beta p_g$ $(p_g=\sqrt{2mU_0})$ since the evolution here is strongly nonlinear. Above the transfer threshold the motion is the superposition of two processes shown in Fig. 2: a slow interdot oscillation with the corresponding frequency ω_L and fast oscillations at the frequencies on the order of $\omega_0 \gg \omega_L$ in the vicinity of the minima not leading to the spin resonance. The increase in the maximum of the momentum p_x compared to the lower-field case, where the transfer is still prohibited and the motion occurs at the frequencies determined by ω_L is on the order of ω_0/ω_L. However, since this very large increase corresponds to the frequencies far away from the Zeeman resonance, it influences the spin dynamics relatively weakly. The momentum Fourier component corresponding to the slow motion is proportional to $\omega_L d$ now, causing the abrupt change in the Rabi frequency. The spin behavior becomes strongly irregular. In Fig. 1(b) we present the corresponding Fourier power spectra in the case of interminimum transfer showing this spin dynamics. If a broader DQD structure is considered then a lower driving field can excite the oscillations with larger electron momentum due to a more extended and smoother confining potential. Here the Rabi frequency of σ^z flip is increased by a factor of 2 when comparing $d=100\sqrt{2}$ and $d=200\sqrt{2}$ nm structures since the interwell transfer is characterized by a factor of 2 greater amplitude of p_x at ω_L. The corresponding phase portraits are presented in Figs. 1(c) and 1(d) for the regular and irregular dynamics shown in Fig. 1. The plot in Fig. 1(d) is a signature of approach to chaotic regime, where the back and forth spin motion on a short-time scale is superimposed by a more regular dynamics leading to the spin flip on the longer time scale. It should be noted that the terms "chaotic motion" together with the "irregular motion" used in the paper refer to the visual shapes of the parameter dy-

namics rather than to a strictly defined dynamical chaos. The possible appearance and investigation of dynamical chaos in our system is outside of the scope of the present paper since our goal here is limited to the observation and description of the transition to irregular dynamics for coupled coordinate and spin degrees of freedom. Hence, we do not perform a too detailed investigation of the dynamical properties including, for example, the analysis of Lyapunov exponent spectrum.[27] Still, the analysis presented above and in Fig. 1 certainly lead to a conclusion that the spin dynamics in our system is strongly affected by the SO coupling and can be tuned by varying both the geometrical parameters of the nanostructure and the amplitude of external electric field.

B. Orbital resonance: $\omega=\omega_0$

Another type of dynamics to be considered is the evolution under the orbital resonance field at the QD oscillation frequency ω_0. When the electric field amplitude is high enough to overcome the barrier and the momentum relaxation, the particle can be driven through both QDs which is shown in Fig. 3(a) for $E_0=1.6$ kV/cm, although a full flip for σ^z is not achieved even if an artificially large $g=4.0$ is considered (dashed lines) as shown in Fig. 3(b). The corresponding Fourier power spectra for $g=-0.45$ are shown in Fig. 3(c). By comparing Figs. 1 and 3, it becomes clear that the expansion in the space motion leads to the enrichment in both coordinate and spin-power spectra due to SO coupling. The dominating part of spectrum is located between the lowest ω_L and the highest ω_0 frequencies of the system which gives rise to various contributions in the whole interval between them. The phase portrait for $[\sigma^y(t),\sigma^z(t)]$ is presented in Fig. 3(d) where one can see that the spin dynamics indeed does not show a full spin flip and is asymmetric with respect to the maximum spin projections since the potential $U(x)$ is spatially asymmetric with respect to the single QD minimum.

The character of the spin evolution changes significantly in a broader DQD structure. Let us consider $d=200\sqrt{2}$ nm which is twice the initial value and the corresponding frequency ω_0 is now factor of 2 lower. By a moderate increase in E_0 from 1.6 to 2.0 kV/cm, one can significantly modify the particle dynamics and, in particular, achieve a full σ^z flip shown in Fig. 3(e). The calculations show that after some period of transient dynamics a steady σ^z oscillations are reached which is further confirmed by the Fourier power spectrum the dominating peak at new ω_0. The corresponding phase portrait for $[\sigma^y(t),\sigma^z(t)]$ with a full spin flip is shown in Fig. 3(e) which in comparison to Fig. 1(d) indicates that the spin evolution here has a more regular character. This can be also confirmed by the analysis of $\sigma^z(t)$ dynamics which shows regular oscillations after the transient period. The results presented above demonstrate again that the evolution of a spin in the presence of SO interaction is very sensitive to the spatial motion and geometrical parameters of the host nanostructure.

To study the long-term effect of the orbital resonance field, a finite length pulse with

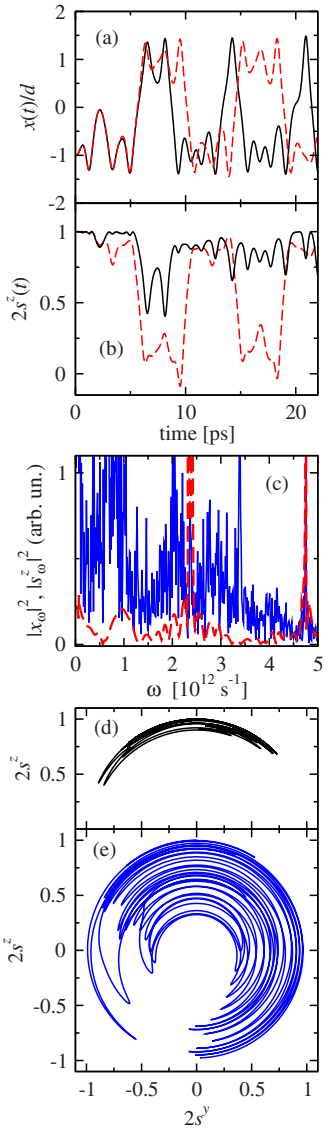

FIG. 3. (Color online) Evolution of (a) $x(t)$ and (b) $\sigma^z(t)$ at the primary resonance $\omega=\omega_0$ and $E_0=1.6$ kV/cm where the particle with $g=-0.45$ (solid black line) and $g=4.0$ (dashed red line) is driven through both QDs. The increase in the g factor leads to a much stronger σ^z modulation. (c) The Fourier power spectra corresponding to $x(t)$ (dashed red line) and $\sigma^z(t)$ (solid blue line) at $g=-0.45$ shown in (a) and (b), respectively. (d) Phase portrait for $\omega=\omega_0$, $d=100\sqrt{2}$ nm, $E_0=1.6$ kV/cm, and time $t<50$ ps. (e) Same for $d=200\sqrt{2}$ nm and $E_0=2.0$ kV/cm, demonstrating the achieved full spin flip.

$$E(t)=E_0\exp\left(-\frac{(t-t_0)^2}{t_P^2}\right)\sin\omega_0 t \tag{9}$$

will be considered. We focus on the asymptotic values at $t\gg t_P$ for $x(t)$ and $\sigma^z(t)$ for the coupled spin-coordinate evolution. Thus, we take $t_0=2t_P$ and t_P varying from $2T_0$ to $12T_0$, where $T_0=2\pi/\omega_0$, and the amplitude $E_0=3$ kV/cm. The results are shown in Fig. 4(a) for the zero magnetic field and in Fig. 4(b) for $B_z=4$ T. It follows from Eq. (4) that at zero magnetic field $\sigma^x\equiv 0$ and for the given initial condition

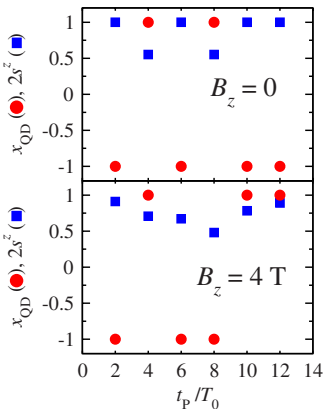

FIG. 4. (Color online) Asymptotic values $x_{QD}=x(t\to\infty)/d$ (filled circles) and $\sigma^z(t\to\infty)$ (filled squares) after the system has been driven by resonant pulses with $E_0=3$ kV/cm and varying duration for (a) $B_z=0$ and (b) $B_z=4$ T. The magnetic field strongly affects both the spin and the coordinate dynamics demonstrating the role of SO coupling.

$x(0)=0$, the solutions for $x(t)$ and $\sigma^y(t),\sigma^z(t)$ are related as

$$\begin{bmatrix} \sigma^y(x) \\ \sigma^z(x) \end{bmatrix} = \begin{bmatrix} \cos(2\beta mx) & -\sin(2\beta mx) \\ \sin(2\beta mx) & \cos(2\beta mx) \end{bmatrix} \begin{bmatrix} \sigma^y(0) \\ \sigma^z(0) \end{bmatrix}. \quad (10)$$

Therefore, the spin returns to the initial state along with the coordinate as it can be seen in Fig. 4(a). When the magnetic field is applied, the spin-orbit $\beta\sigma^x\hat{p}_x$ and Zeeman $(g/2)\mu_B\sigma^z B_z$ terms in Eq. (5) do not commute, and such relation is no longer valid. Here, both the final $x(t)$ and $\sigma^z(t)$ values form a different pattern shown in Fig. 4(b). We emphasize that not only the spin but the coordinate asymptotic also becomes magnetic-field dependent due to the SO coupling term $\beta\sigma^x$ in the velocity, as it can be seen by comparing Figs. 4(a) and 4(b). This result is an important complementary effect of the influence of spin dynamics on the charge evolution which should be taken into account when both the charge and spin dynamics in systems with strong spin-orbit coupling are of interest.

IV. CONCLUSIONS

We have studied in the semiclassical approximation-coupled coordinate-spin dynamics of electron in a one-dimensional double quantum dot with the Dresselhaus type of SO coupling in external magnetic field. The considered system was driven by a harmonic electric field with the frequency matching the transition between the orbital levels of the quantum dot or the Zeeman resonance or by an intense finite-time orbital resonant-field pulse. The increase in the field amplitude makes the electron transfer between the potential minima possible and triggers strongly irregular behavior in both coupled charge and spin channels. These irregularities in the spin motion suggest that in a nonlinear system evolution of spin coupled to the momentum is very sensitive to the spatial motion. The spin flips, therefore, cannot be well described by a single Rabi frequency. In turn, the anomalous spin-dependent contribution to the electron velocity leads to the position time dependence $x(t)$ strongly different from that expected for the zero spin-orbit coupling. The study of the development of these irregularities into the real chaos in the spin subsystem, involving the nontrivial Lyapunov spectrum analysis, is an interesting problem for the future research. The geometry of the nanostructure strongly influences the spin dynamics in this nonlinear regime. These conclusions emphasize the importance of the possible nonlinear behavior for the initialization and manipulation of spin states in quantum dots in the experimentally accessible range of system parameters.

ACKNOWLEDGMENTS

E.Y.S. acknowledges support by the Ikerbasque Foundation and the University of Basque Country (Grant No. GIU07/40). D.V.K. is grateful to V. A. Burdov and A. I. Malyshev for helpful discussions and is supported by the RNP Program of Ministry of Education and Science RF (Grants No. 2.1.1.2686, No. 2.1.1.3778, and No. 2.2.2.2/4297), by the RFBR (Grant No. 09-02-1241-a), and by the USCRDF (Grant No. BP4M01).

[1] M. Valin-Rodriguez, A. Puente, L. Serra, and E. Lipparini, Phys. Rev. B **66**, 235322 (2002).
[2] L. S. Levitov and E. I. Rashba, Phys. Rev. B **67**, 115324 (2003).
[3] L. Meza-Montes, C. F. Destefani, and S. E. Ulloa, Phys. Rev. B **78**, 205307 (2008).
[4] G. Burkard, D. Loss, and D. P. DiVincenzo, Phys. Rev. B **59**, 2070 (1999).
[5] E. I. Rashba and V. I. Sheka, Fiz. Tverd. Tela (Leningrad) **3**, 2369 (1961) [Sov. Phys. Solid State **3**, 1718 (1962)]; in *Landau Level Spectroscopy*, edited by G. Landwehr and E. I. Rashba, (North-Holland, Amsterdam, 1991), p. 131, and references therein.
[6] E. I. Rashba and Al. L. Efros, Phys. Rev. Lett. **91**, 126405 (2003); Appl. Phys. Lett. **83**, 5295 (2003).
[7] D. V. Bulaev and D. Loss, Phys. Rev. Lett. **98**, 097202 (2007); M. Duckheim and D. Loss, *ibid.* **101**, 226602 (2008).
[8] D. V. Khomitsky, Phys. Rev. B **77**, 113313 (2008); **79**, 205401 (2009).
[9] K. C. Nowack, F. H. L. Koppens, Yu. V. Nazarov, and L. M. K. Vandersypen, Science **318**, 1430 (2007).
[10] M. Pioro-Ladriere, T. Obata, Y. Tokura, Y.-S. Shin, T. Kubo, K. Yoshida, T. Taniyama, and S. Tarucha, Nat. Phys. **4**, 776 (2008).
[11] L. P. Rokhinson, V. Larkina, Y. B. Lyanda-Geller, L. N. Pfeiffer, and K. W. West, Phys. Rev. Lett. **93**, 146601 (2004).
[12] J. Schliemann, D. Loss, and R. M. Westervelt, Phys. Rev. Lett. **94**, 206801 (2005).
[13] A. A. Reynoso, G. Usaj, and C. A. Balseiro, Phys. Rev. B **78**, 115312 (2008); V. Ya. Demikhovskii, G. M. Maksimova, and E. V. Frolova, *ibid.* **78**, 115401 (2008).

[14] O. Zaitsev, D. Frustaglia, and K. Richter, Phys. Rev. Lett. **94**, 026809 (2005); Phys. Rev. B **72**, 155325 (2005).
[15] Y. Tserkovnyak and S. Akhanjee, Phys. Rev. B **79**, 085114 (2009).
[16] P. Stano and J. Fabian, Phys. Rev. Lett. **96**, 186602 (2006); Phys. Rev. B **72**, 155410 (2005); **74**, 045320 (2006).
[17] Y. G. Semenov and K. W. Kim, Phys. Rev. Lett. **92**, 026601 (2004); Phys. Rev. B **75**, 195342 (2007).
[18] B. V. Chirikov, Phys. Rep. **52**, 263 (1979).
[19] L. E. Reichl and W. M. Zheng, Phys. Rev. A **29**, 2186 (1984).
[20] W. A. Lin and L. E. Ballentine, Phys. Rev. Lett. **65**, 2927 (1990); Phys. Rev. A **45**, 3637 (1992).
[21] D. Sánchez and L. Serra, Phys. Rev. B **74**, 153313 (2006); M. Crisan, D. Sánchez, R. López, L. Serra, and I. Grosu, *ibid.* **79**, 125319 (2009).
[22] C. Lü, U. Zülicke, and M. W. Wu, Phys. Rev. B **78**, 165321 (2008).
[23] C. L. Romano, P. I. Tamborenea, and S. E. Ulloa, Phys. Rev. B **74**, 155433 (2006).
[24] For electrons, M. I. Dyakonov and V. Yu. Kachorovskii, Fiz. Tekh. Poluprovodn. (S.-Peterburg) **20**, 178 (1986) [Sov. Phys. Semicond. **20**, 110 (1986)]; For electrons and holes, E. I. Rashba and E. Ya. Sherman, Phys. Lett. A **129**, 175 (1988); For holes in quantum wires, D. Csontos, P. Brusheim, U. Zulicke, and H. Q. Xu, Phys. Rev. B **79**, 155323 (2009).
[25] A. V. Khaetskii and Y. V. Nazarov, Phys. Rev. B **61**, 12639 (2000); J. L. Cheng, M. W. Wu, and C. Lu, *ibid.* **69**, 115318 (2004).
[26] Z. Yang, S. Zhang, and Y. C. Li, Phys. Rev. Lett. **99**, 134101 (2007).
[27] A. J. Lichtenberg and M. A. Lieberman, *Regular and Stochastic Motion* (Springer-Verlag, Berlin, 1983).